Quantitative Proteomic Analysis of Sokotrasterol Sulfate-stimulated Primary Human Endothelial Cells*[S]

Aly Karsan‡§¶, Ingrid Pollet‡, Li-Rong Yu¶, King C. Chan¶, Thomas P. Conrads¶, David A. Lucas¶, Raymond Andersen‖, and Timothy Veenstra¶

The endothelium forms a continuous monolayer at the interface between blood and tissue and contributes significantly to the sensing and transducing of signals between blood and tissue. New blood vessel formation, or angiogenesis, is initiated by the activation of endothelial cells and is an important process required for various pathological and physiological situations. This study used cleavable isotope-coded affinity tag reagents combined with mass spectrometry to investigate the molecular basis of a recently discovered angiogenesis-promoting steroid, sokotrasterol sulfate. Changes in the relative abundances of over 1000 proteins within human endothelial cells treated with sokotrasterol sulfate and vehicle-treated cells were identified and quantitated using this technique. A method that examines the entire ensemble of quantitative measurements was developed to identify proteins that showed a statistically significant change in relative abundance resulting from treatment with sokotrasterol sulfate. A total of 93 proteins was significantly up-regulated, and 37 were down-regulated in response to sokotrasterol sulfate stimulation of endothelial cells. Among the up-regulated proteins, several were identified that are novel to endothelial cells and are likely involved in cell communication and morphogenesis. These findings are consistent with a role for sokotrasterol sulfate in endothelial sprouting. ***Molecular & Cellular Proteomics 4: 191–204, 2005.***

Angiogenesis, the formation of new blood vessels from existing vessels, is a complex process requiring modulation of multiple endothelial cell functions (1, 2). Endothelial cells line the interior of blood vessels and are responsible for initiating the growth of new vessels (1, 2). The formation of capillary sprouts from the existing microvasculature occurs secondary to an inciting stimulus resulting in increased vascular permeability, accumulation of extravascular fibrin, and local proteolytic degradation of the basement membrane (1, 2). The endothelial cells overlying the disrupted region become activated, change shape, and extend elongated processes into the surrounding tissue (1, 2). Directed migration toward the angiogenic stimulus results in the formation of a column of endothelial cells (1, 2). Just proximal to the migrating tip of the column is a region of proliferating cells that cause the sprout to increase in length (1, 2). Proximal to the proliferative zone, the endothelial cells undergo a second shape change, adhere tightly to each other, and begin to form a lumen resulting in a capillary plexus (1, 2). Fusion of individual sprouts at their tips closes the loop and circulates blood into the vascularized area (1, 2). Throughout this process the expression of various proteins is tightly regulated (1, 2).

The development of new blood vessels is required in various pathological and physiological processes including embryogenesis, organogenesis, ovarian follicle development, and tumor growth and metastasis (1, 3). Ischemic coronary artery disease is a major cause of morbidity and the leading cause of mortality in the industrialized world (4). The major reason for cardiovascular disease is the occlusion of blood vessels due to atherosclerosis (4). Neovascularization, or new blood vessel growth, is also required to bypass the occlusion of arteries caused by atherosclerosis (4). The effects of neovascularization in ischemic disease may be both beneficial and detrimental to the patient (5, 6). Lack of adequate neovascularization when arteries narrow can result in clinical symptoms of ischemia, and strategies to promote angiogenesis may improve symptoms and tissue function (7). In contrast, neovascularization of an atherosclerotic plaque can result in growth of the plaque and further luminal stenosis, or plaque hemorrhage and rupture (8, 9). While the beneficial effects of using angiogenic drugs to promote neovascularization in ischemic disease remains controversial, several clinical trials are under way to evaluate the benefits (9).

In an attempt to identify small molecules with the ability to stimulate blood vessel growth for potential use in therapeutic angiogenesis, we recently screened a library of crude marine extracts and identified a sulfated steroid called sokotrasterol

From the ‡Department of Medical Biophysics and Pathology and Laboratory Medicine, British Columbia Cancer Agency, Vancouver, British Columbia V5Z 1L3, Canada, ¶Laboratory of Proteomics and Analytical Technologies, SAIC-Frederick, Inc., NCI, National Institutes of Health, Frederick, Maryland 21702-1201, and ‖Department of Chemistry, University of British Columbia, Vancouver, British Columbia V6T 1Z4, Canada

Received, October 7, 2004, and in revised form, December 12, 2004

Published, MCP Papers in Press, December 20, 2004, DOI 10.1074/mcp.M400152-MCP200

sulfate (10).[1] Sokotrasterol sulfate stimulation causes sprouting of endothelial cells *in vitro* in a dose-dependent manner and induces the development of new blood vessels in an *in vivo* chick chorioallantoic membrane model of angiogenesis. To ensure the safe use of angiogenic therapies, however, a thorough understanding of the mechanisms of neovascularization is important. To understand how sokotrasterol sulfate affects the endothelial cell and potentially understand its mechanism of angiogenic action, differential protein analysis using cleavable isotope-coded affinity tag (cICAT)[2] reagents combined with mass spectrometry (11) was used to quantitate protein expression differences in primary human endothelial cells stimulated with sokotrasterol sulfate. In addition, a statistical analysis was performed to determine what magnitude of change in relative abundance between proteins extracted from the treated and control human umbilical vein endothelial cells (HUVECs) was significant. Previous studies using ICAT have arbitrarily selected a specific cut-off as a measure of significance; however, the results presented in this study show that the level of significance is likely to be different for every data set analyzed in this manner. In particular, membrane proteins such as Tie-1 and the α_v integrin that are known to be required in the developing vasculature were shown to be up-regulated at the borderline level, bolstering the requirement for choosing optimal cut-off levels for up- and down-regulated proteins. Several other proteins, such as Dysferlin and E2F4, demonstrated borderline but significant up-regulation by sokotrasterol sulfate implicating these proteins in the process of angiogenesis induced by sokotrasterol sulfate.

EXPERIMENTAL PROCEDURES

Materials—Ammonium bicarbonate (NH_4HCO_3), ammonium formate (NH_4HCO_2), guanidine hydrochloride, dibasic sodium phosphate (Na_2HPO_4), monobasic sodium phosphate (NaH_2PO_4), sodium chloride (NaCl), ammonium hydroxide (NH_4OH), Tris, sodium fluoride (NaF), sodium orthovanadate (Na_3VO_4), Triton X-100, and phenylmethylsulfonyl fluoride were purchased from Sigma. Trifluoroacetic acid and formic acid were obtained from Fluka (Milwaukee, WI). High performance liquid chromatography grade acetonitrile (CH_3CN) and methanol (CH_3OH) were obtained from EM Science (Darmstadt, Germany). UltraLink™ immobilized monomeric avidin, Tris(2-carboxyethyl)phosphine hydrochloride, ImmunoPure D-biotin, and bicinchonic acid (BCA) protein assay reagent kit were purchased from Pierce. Water was purified by a Barnstead Nanopure system (Dubuque, IA). Cleavable ICAT reagents were purchased from Applied Biosystems, Inc. (Foster City, CA).

Cell Culture—Primary HUVECs were isolated and cultured as described previously (12). Three 10-cm tissue culture plates of confluent HUVECs (~1.5×10^7 cells) were treated for 24 h with either sokotrasterol sulfate (5 μg/ml) or vehicle (dimethyl sulfoxide (Me_2SO)). After 24 h, HUVECs were washed twice with cold PBS and lysed directly on the plates with 50 mM Tris-HCl (pH 8.5), 2% Triton X-100, 10 mM NaF, 1 mM Na_3VO_4, and phenylmethylsulfonyl fluoride, and material from each condition was scraped into a 1.5-ml tube and sonicated on ice.

Cleavable ICAT Labeling—Equal amounts of HUVEC protein extracts (500 μg each) were labeled either with the light (control, cICAT-$^{13}C_0$) or the heavy (sokotrasterol sulfate-treated, cICAT-$^{13}C_9$) isotopomeric versions of the cICAT reagent using a modified method from that recommended by the manufacturer (13). Briefly 500 μg of each HUVEC cell protein extract was dissolved in 400 μl of 6 M guanidine hydrochloride in 50 mM NH_4HCO_3, pH 8.3. Each sample was chemically reduced by adding 5 μl of 100 mM Tris(2-carboxyethyl)phosphine hydrochloride followed by boiling in a water bath for 10 min. The reduced samples were transferred to vials containing either cICAT-$^{13}C_0$ or cICAT-$^{13}C_9$ dissolved in 20 μl of CH_3CN and incubated at 37 °C for 2 h. The two samples were combined, buffer-exchanged into 50 mM NH_4HCO_3, pH 8.3, using a D-Salt Excellulose plastic desalting column (Pierce), and digested with trypsin (Promega, Madison, WI) overnight at 37 °C using an enzyme to protein ratio of 1:50 (w/w). The digestion was quenched by boiling the samples in a water bath for 10 min and adding phenylmethylsulfonyl fluoride to a final concentration of 1 mM.

Affinity Purification and Cleaving of cICAT-labeled Peptides—A 1.5-ml bed volume UltraLink immobilized monomeric avidin column was slurry-packed in a glass Pasteur pipette and equilibrated with 2× PBS (0.2 M sodium phosphate, 0.3 M NaCl, pH 7.2). The column was blocked with 2 mM D-biotin in 2× PBS, pH 7.2, the biotin was stripped from the reversible binding sites of the column according to the manufacturer's instructions, and the column was re-equilibrated with 2× PBS, pH 7.2. The cICAT-labeled peptides were boiled for 5 min, cooled to room temperature, loaded onto the avidin column, and incubated for 15 min at ambient temperature. After washing the column with 10 bed volumes each of 2× PBS, pH 7.2; 1× PBS, pH 7.2; and 50 mM NH_4HCO_3, pH 8.3, 20% CH_3CN, the cICAT-labeled peptides were eluted using 30% CH_3CN, 0.4% formic acid and lyophilized to dryness. The biotin moiety was cleaved from the cICAT-labeled peptides by treatment with the cleaving reagents provided by the manufacturer for 2 h at 37 °C and lyophilized to dryness.

Strong Cation Exchange Fractionation of cICAT-labeled Peptides—The lyophilized HUVEC cICAT-labeled peptides were dissolved in 170 μl of 0.1% formic acid, 25% CH_3CN and injected onto a strong cation exchange liquid chromatography (SCXLC) column (1 mm × 150 mm, polysulfoethyl A, PolyLC Inc., Columbia, MD). The following NH_4HCO_2/CH_3CN multistep gradient was used to elute the cICAT-labeled peptides from the column at a flow rate of 50 μl/min: 2% mobile phase B for 8 min followed by a linear increase to 10% B in 32 min, then a linear increase to 60% B in 45 min, a steep increase to 100% B in 1 min, and maintenance at 100% B for 10 min. Mobile phase A was 25% CH_3CN, and mobile phase B was 25% CH_3CN, 0.5 M NH_4HCO_2, pH 3.0. Fractions were collected every minute for 96 min. Each SCXLC fraction was lyophilized and reconstituted in 20 μl of 0.1% trifluoroacetic acid prior to microcapillary reversed-phase (μRP) LC-MS/MS.

Microcapillary Reversed-phase LC-MS/MS of cICAT-labeled Peptides—Ten-centimeter-long μRPLC-electrospray ionization (ESI) columns were coupled on line with an ion trap mass spectrometer (LCQ Deca XP, ThermoElectron, San Jose, CA) to analyze the cICAT-labeled peptides extracted from the control and sokotrasterol sulfate-treated HUVECs. To construct the 10-cm-long μRPLC-ESI columns, 75-μm-inner diameter fused silica microcapillaries (Polymicro Tech-

[1] A. Karsan, I. Pollet, T. P. Conrads, R. Andersen, and T. Veenstra, manuscript in preparation.

[2] The abbreviations used are: cICAT, cleavable isotope-coded affinity tag; MS, mass spectrometry; HUVEC, human umbilical vein endothelial cell; SCXLC, strong cation exchange liquid chromatography; μRP, microcapillary reversed-phase; ESI, electrospray ionization; PBS, phosphate-buffered saline; LC, liquid chromatography; MS/MS, tandem mass spectrometry; ALCAM, activated leucocyte cell adhesion molecule.

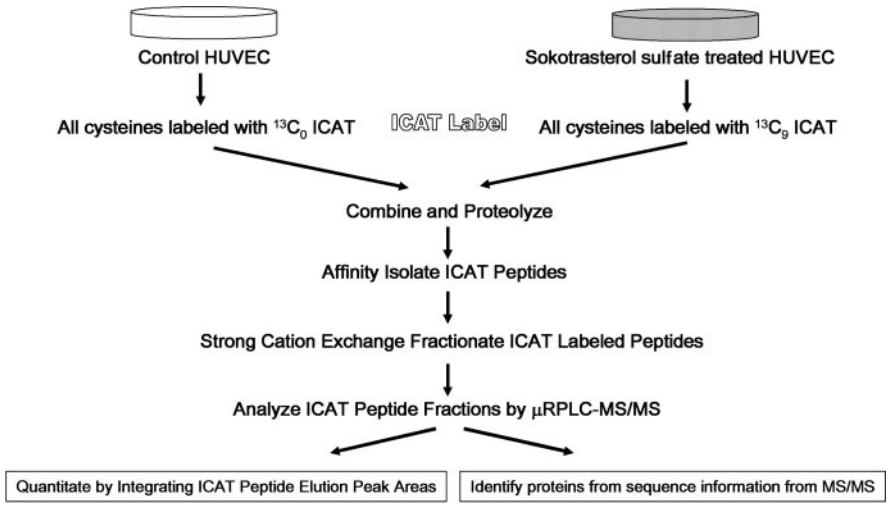

FIG. 1. **Schema of ICAT approach using SCXLC and μRPLC-MS/MS.**

nologies, Phoenix, AZ) were flame-pulled to construct a fine inner diameter (*i.e.* 5–7 μm) tip against which 3-μm, 300-Å pore size C_{18} silica-bonded stationary reversed-phase particles (Vydac) were slurry-packed using a slurry packing pump (Model 1666, Alltech Associates, Deerfield, IL). The columns were connected via a stainless steel union to an Agilent 1100 capillary LC system (Agilent Technologies, Palo Alto, CA), which was used to deliver mobile phases A (0.1% formic acid in water) and B (0.1% formic acid in CH_3CN). After loading 6 μl of sample, the cICAT-labeled peptides were eluted at a flow rate of ~400 nl/min using a linear step gradient of 2–40% B for 110 min and 40–98% B for 30 min. The ion trap mass spectrometer was operated in a data-dependent MS/MS mode in which the three most intense peptide molecular ions in the MS scan were sequentially and dynamically selected for subsequent collision-induced dissociation using a normalized collision energy of 35%. The MS spectrum for the molecular ions was acquired using two microscans for the mass range of *m/z* 475–2000, and the collision-induced dissociation spectrum for the fragment ions was acquired using three microscans. In this analysis the following manufacturer-recommended settings were used: the maximum ion injection time permitted was 75 ms for each of the MS and MS/MS microscans with a maximum arbitrary ion target value of 1×10^8 for MS and 5×10^7 for MS/MS acquisitions. Therefore, the *maximum* cycle time in between MS acquisitions was ~825 ms. The voltage and temperature for the capillary of the ion source were set at 10 V and 160 °C, respectively.

Peptide Identification and Quantitation—The raw MS/MS data acquired on the ion trap mass spectrometer were searched using SEQUEST against the *Homo sapiens* proteome data base (28,816 entries) downloaded from the European Bioinformatics Institute (EBI) (www.ebi.ac.uk/proteome/index.html). The Archaea-derived data base (12,038 entries) utilized in the false-positive bioinformatic analysis was constructed using genomic sequence information from the following organisms: *Aeropyrum pernix*, *Archaeoglobus fulgidus*, *Pyrobaculum aerophilum*, *Sulfolobus tokodaii*, and *Thermoplasma volcanium*. Dynamic modifications for cysteinyl (Cys) residues were set by mass additions of the cleaved cICAT labels (227.13 Da for the light label and 236.16 Da for the heavy label) in a single search. SEQUEST criteria were set as $X_{corr} \geq 1.9$ for $[M + H]^{1+}$ ions, ≥ 2.2 for $[M + 2H]^{2+}$ ions, and ≥ 2.9 for $[M + 3H]^{3+}$ ions and as $\Delta C_n \geq 0.08$ for the identification of fully tryptic peptides within the cICAT-labeled samples. The identified peptides were quantified using XPRESS (ThermoElectron), which calculates the relative abundances ($^{13}C_9/^{13}C_0$ in this data set) of peptides based on the area of their extracted ion chromatograms.

RESULTS

Various steroid compounds have been shown to have either pro- or antiangiogenic activity, but the mechanism by which these steroids function remains to be elucidated (14). There is some suggestion that estradiol functions by promoting the synthesis and release of other angiogenic factors to promote neovascularization (15, 16). The identification of a novel function for the sulfated steroid sokotrasterol sulfate prompted us to attempt to understand its mechanism of action. There is no information currently on the effect of sokotrasterol sulfate on the molecular profile of any cell type. Since the sprouting of new vessels is initiated at the level of the endothelial cell, primary human endothelial cells were treated with sokotrasterol sulfate or vehicle (Me_2SO) to quantitate differential protein expression between these two conditions.

Crude protein extracts harvested from HUVECs treated with Me_2SO as a control or with sokotrasterol sulfate (5 μg/ml) for 24 h were prepared and separately labeled (Fig. 1) with the isotopomerically distinct versions of the cICAT reagents (cICAT-$^{13}C_0$ and cICAT-$^{13}C_9$). Both versions of the cICAT reagent contain a thiol-reactive group and a biotin moiety separated by a linker region in which the heavy version contains nine ^{13}C atoms in place of nine ^{12}C atoms in the light version. After cICAT labeling, the protein extracts were combined and digested with trypsin, and the cICAT-modified peptides were recovered using immobilized avidin chromatography. The cICAT-labeled tryptic peptides were resolved into 96 fractions by SCXLC that were subsequently analyzed by data-dependent μRPLC-MS/MS.

Central to comprehensive proteomic measurements is the ability to identify large numbers of peptides, hence proteins. It is generally accepted that no single chromatographic or electrophoretic procedure is capable of resolving the complex mixture of peptides that results from a global proteolytic digest of a proteome. Therefore, combining two or more orthogonal separation procedures dramatically improves the overall

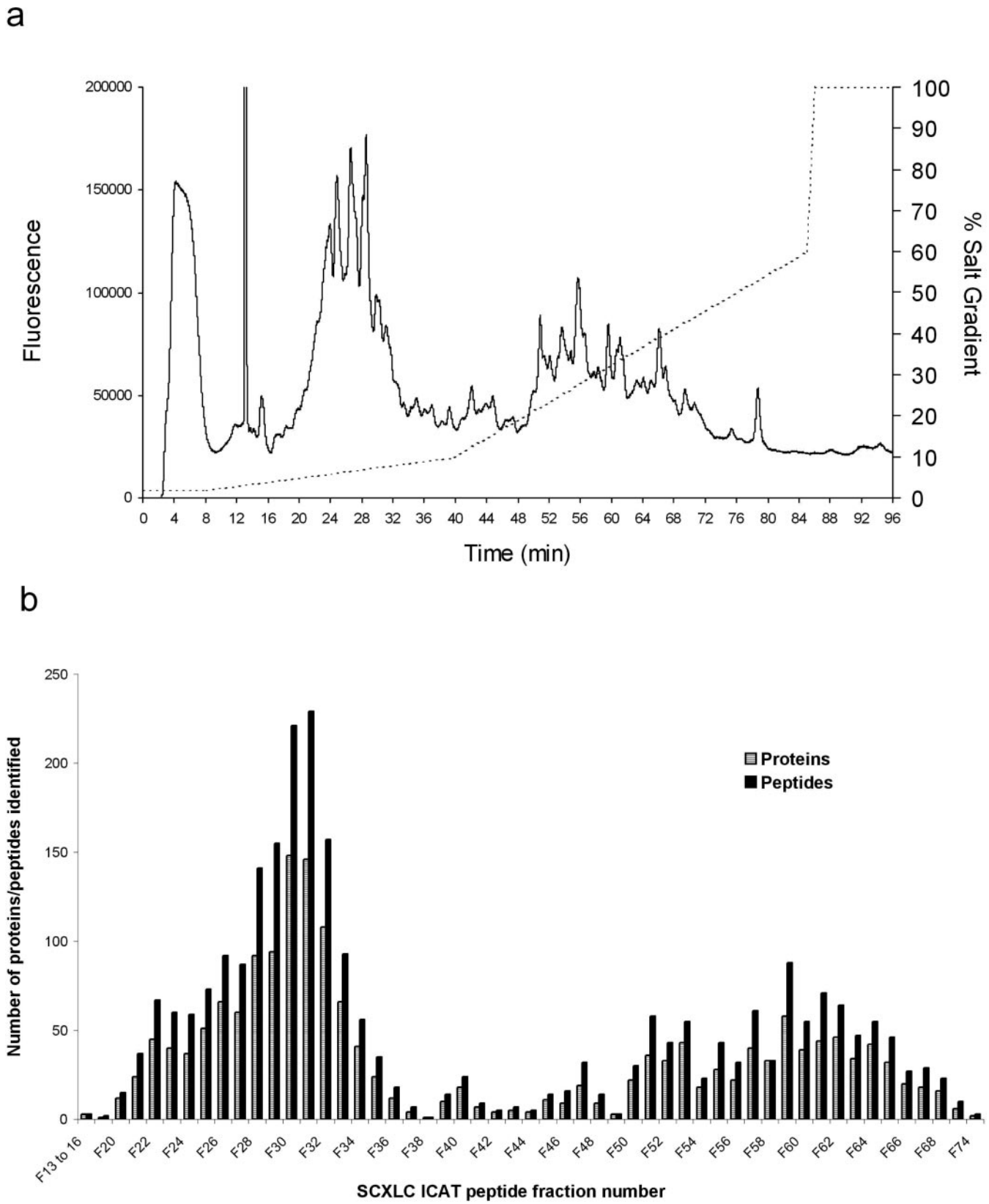

FIG. 2. **Separation of cICAT-labeled peptides by SCXLC.** *a*, fluorescence chromatogram of cICAT-labeled peptides separated by SCXLC. *b*, histogram illustrating the number of peptides (*hatched bars*) and proteins (*solid bars*) identified in the μRPLC-MS/MS analysis of the SCXLC fractions.

peak capacity of the measurement and results in larger numbers of peptides being identified from complex proteome digests (17). Fractionation is a critical aspect of successful global proteome investigations that utilize MS because while a mass spectrometer can perform mass measurements on several co-eluting peptides, conventional MS/MS cycle times for most instruments typically enable only a limited number of these peptides to be selected for collision-induced dissociation. Therefore, limiting the number of co-eluting peptides helps to increase the percentage of species that may be identified. Illustrated in Fig. 2*a* is the SCXLC chromatogram of the cICAT-labeled peptide digest from HUVECs. Fig. 2*b* depicts a histogram of the peptides and proteins identified in each μRPLC-MS/MS analysis of the 96 SCXLC fractions. There is good correlation between the number of peptides/proteins identified and the apparent fluorescence intensities of each of the SCXLC cICAT fractions. In total, 2162 unique cICAT-labeled peptides, corresponding to 1019 proteins, from HUVECs treated with vehicle or sokotrasterol sulfate were quantitated in this study (Supplemental Table I). Although the SEQUEST analysis resulted in 2162 uniquely identified peptides, some portion of these peptides may identify more than one protein due to sequence homology among orthologous proteins etc. Hence we have conducted a more detailed search of the peptides and proteins identified to account for these homology effects and find that 1602 peptides (74.1%) are found to uniquely identify a single protein and 560 (25.9%) peptides identify more than one protein (*i.e.* protein clusters) due to peptide sequence redundancy (*i.e.* 100% homology in more than one protein in the data base).

The ability to identify a protein depends directly on the extent to which the peptide identified possesses a unique sequence amid all proteins in the genome-derived data base. The rate of false-positive peptide (hence protein) identifications in "bottom-up" proteomic approaches is multifactorial with strong dependence on almost every aspect of the experimental execution. Such factors governing false-positive identifications include the quality and specificity of the proteolytic digest, the calibration and operation of the mass spectrometer, the bioinformatic algorithm used to search the MS-derived data, the interpretation of the bioinformatic output, and the accuracy and completeness of the genome-derived proteomic data base. It is thus necessary that proteomic data sets derived from the aforementioned experimental approach be subjected to false-positive analyses to determine the confidence of the reported peptide (protein) identifications. A false-positive analysis of the peptide (protein) identifications was conducted by searching the data from the μRPLC-MS/MS analyses of the SCXLC cICAT peptide fractions against an Archaea-derived proteomic data base utilizing identical bioinformatic filters for peptide identification (see "Experimental Procedures"). This false-positive analysis resulted in the identification of 22 unique peptides from the Archaea-derived proteomic data base as compared with 2162

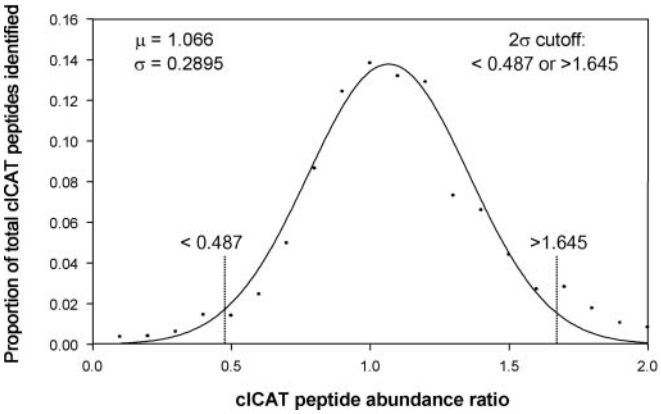

FIG. 3. **Analysis to determine significant differentially expressed proteins.** Shown is the plot of the proportion of total cICAT-labeled peptides identified as a function of their measured abundance ratios ($^{13}C_9/^{13}C_0$). The cut-off points of peptides whose abundance ratios were 2σ below (0.487) or above (1.645) the mean in response to sokotrasterol sulfate stimulation of endothelial cells are demarcated by a *dashed vertical line*.

unique peptides from the human proteomic data base. We therefore estimate a false-positive rate of 1% (percentage of false-positives = (22/2162) × 100) for the present cICAT peptide data set that reflects the high stringency of the SEQUEST scoring and filtering parameters used in this analysis.

The relative abundances of the cICAT-labeled peptides were quantified based on the area of their extracted ion chromatograms reconstructed from the molecular ion MS scans of the $^{13}C_9/^{13}C_0$ variants of each peptide. There can be no standard for what changes in relative abundance as measured by cICAT analyses represent statistically significant changes in peptide abundance ratios since the determination of cICAT ratios depends directly on multiple experimental factors. These include factors such as the extent to which the initial mixing of samples was equal, the relative efficiency of recovery of each of the cICAT peptide pairs from the sample preparation, the inherent resolution and accuracy of the MS instrumentation utilized, and the number of molecular ion scans across each cICAT peptide pair μRPLC peak. We sought to determine the threshold above and below which the measured cICAT peptide abundance ratios were statistically significant within this data set. The normalized percentage of the number of cICAT-labeled peptides identified within binned abundance ratios (*e.g.* 1.0–1.09, 1.1–1.19, etc.) was plotted (Fig. 3). Theoretically the distribution of the ICAT ratios should be a normal distribution defined as Equation 1,

$$P = \frac{1}{\sigma\sqrt{2\pi}} e^{-(x-\mu)^2/(2\sigma^2)} \qquad \text{(Eq. 1)}$$

where P is the normalized peptide percentage at a given cICAT peptide pair ratio x, μ is defined as the experimentally measured mean value of the total population of cICAT peptide pair ratios, and σ is standard deviation. The z score is defined as $z = (x - \mu)/\sigma$. Using a non-linear least squares regression

TABLE I
Proteins with increased expression levels in response to sokotrasterol sulphate

Protein name[a]	Swiss-Prot accession no.	-Fold increase in protein levels[b]
14-3-3 protein ζ/δ	P29312	1.74 (5)
180-kDa transmembrane PLA2 receptor	Q13018	3.03
2-Oxoglutarate dehydrogenase E1 component, mitochondrial precursor	Q02218	1.75
60 S acidic ribosomal protein P0	P05388	1.78 (5)
60 S ribosomal protein L10a	P53025	3.80 (4)
Acidic leucine-rich nuclear phosphoprotein 32 family member A	P39687	3.33
Actin filament-associated protein	Q9HBY1	2.78
Adapter-related protein complex 2 α1 subunit	O95782	1.77 (7)
Adenine phosphoribosyltransferase	P07741	1.79
ADP-ribosylation factor 6	P26438	7.69
Alcohol dehydrogenase ($NADP^+$)	P14550	1.65 (5)
Annexin A5	P08758	2.33
Aspartate aminotransferase, cytoplasmic	P17174	3.57
ATP-dependent RNA helicase A	Q08211	1.96 (2)
β-Arrestin 1	P49407	3.57
Bifunctional aminoacyl-tRNA synthetase	P07814	2.24 (7)
Calcium-transporting ATPase type 2C, member 1	P98194	2.44
CD166 antigen precursor	Q13740	2.70
CDC16	Q96AE6	2.38
Chloride intracellular channel protein 1	O00299	2.51 (13)
Cofilin, non-muscle isoform	P23528	1.90 (16)
Contactin-associated protein 1 precursor	P78357	2.44
CTL2 gene	Q8IWA5	2.04
Cytosolic acetoacetyl-coenzyme A thiolase	Q16146	2.13
D-3-Phosphoglycerate dehydrogenase	O43175	1.82
Dihydropteridine reductase	P09417	3.03
Dihydroxyacetone phosphate acyltransferase	O15228	2.50
DNA mismatch repair protein Msh2	P43246	4.35
DNA-dependent protein kinase catalytic subunit	P78527	1.73 (19)
Down syndrome critical region protein 2	O95456	1.67 (2)
Dysferlin	O75923	1.75 (2)
Eukaryotic translation initiation factor 3 subunit 9	P55884	2.14 (4)
Exocyst complex component Sec10	O00471	2.78
FLJ00365 protein	Q8NF37	7.10 (2)
Follistatin-related protein 1 precursor	Q12841	1.77 (3)
Glutamate dehydrogenase 1, mitochondrial precursor	P00367	1.94 (4)
Glutathione peroxidase 1	P07203	1.87 (3)
Glyceraldehyde-3-phosphate dehydrogenase, muscle	P00354	3.19 (17)
Group X secretory phospholipase A2 precursor	O15496	100.0 (2)
Heat shock-related 70-kDa protein 2	P54652	1.75
Hedgehog-interacting protein (hypothetical protein)	Q96QV1	1.75
Homeobox protein HB9	P50219	12.50
Human full-length cDNA clone CS0DC022YA24 of neuroblastoma (fragment)	Q86U01	1.72
Hypothetical protein	O95328	1.82 (2)
Hypothetical protein (fragment)	Q8N3G2	1.72
Hypothetical protein (putative α-mannosyltransferase)	Q9BV10	2.56
Hypothetical protein CGI-99	Q9Y224	1.89
Hypothetical protein FLJ12647	Q9H9N0	1.92
Hypothetical protein FLJ12960	Q9H974	3.33
Hypothetical protein FLJ20397	Q86Y56	2.16 (4)
Hypothetical protein FLJ32019	Q96MR1	2.08
Hypothetical protein KIAA0095	Q14705	3.45
Hypothetical protein KIAA0763	O94863	9.09
Hypothetical protein KIAA1440 (fragment)	Q9P2A8	1.72 (2)
Integrin α_v precursor	P06756	1.65 (3)
Isocitrate dehydrogenase (NADP), cytoplasmic	O75874	1.92
Laminin β-1 chain precursor	P07942	2.28 (5)
Laminin γ-1 chain precursor	P11047	2.27
Leucine-rich glioma-inactivated protein 1 precursor	O95970	16.25 (3)

TABLE I—*continued*

Protein name[a]	Swiss-Prot accession no.	-Fold increase in protein levels[b]
Mitochondrial 60 S ribosomal protein L3	P09001	1.72 (2)
Multisynthetase complex auxiliary component p43	Q12904	1.89 (3)
Myosin heavy chain, non-muscle type A	P35579	2.10 (14)
Myosin light chain alkali, non-muscle isoform	P16475	1.75 (2)
N-Acetylglucosamine-6-sulfatase precursor	P15586	6.25
NUP196 nucleoporin	Q8WYB0	2.27
P2X purinoceptor 4	Q99571	1.82
PP5242	Q8WY64	100.00
Probable serine protease HTRA4 precursor	P83105	5.00
Protein transport protein SEC61 β subunit	P38391	1.75
Protein-tyrosine phosphatase β precursor	P23467	1.69
RanBP7/importin 7	O95373	1.68 (3)
Ran GTPase-activating protein 1	P46060	1.72 (3)
Ras GTPase-activating protein 1	P20936	1.96
Ras-related protein Rab-2A	P08886	2.08
SAM domain and HD domain-containing protein 1	Q9Y3Z3	1.89 (2)
Similar to ubiquitin-protein isopeptide ligase (E3)	Q8TC15	7.14
Small nuclear ribonucleoprotein Sm D3	P43331	2.00
S phase kinase-associated protein 1A	P34991	2.44
Splicing factor U2AF 35-kDa subunit	Q01081	1.81 (4)
SUPT5H protein	O00267	1.81 (4)
SWI/SNF complex 155-kDa subunit	Q92922	3.03
Symplekin	Q92797	2.38
Thioredoxin domain-containing protein 5 precursor	Q8NBS9	1.96 (45)
Transcription factor E2F4	Q16254	1.75
Transducin β-like 2 protein	Q9Y4P3	1.67
Transcriptional coactivator tubedown-100	Q8NEV2	1.96
Translation initiation factor eIF-2B δ subunit	Q9UI10	1.67
Triose-phosphate isomerase	P00938	5.28 (23)
Tumor differentially expressed 1 protein-like	Q9NRX5	25.00
Tyrosine-protein kinase receptor Tie-1 precursor	P35590	1.72 (2)
Uridine 5′-monophosphate synthase	P11172	1.78 (2)
Vacuolar ATP synthase subunit B, kidney isoform	P15313	1.92
Vezatin	Q9HBM0	1.69

[a] PLA2, phospholipase A2; eIF, eukaryotic initiation factor; HD, histidine aspartate; SAM, sterile alpha motif.
[b] Number of peptides identified is shown in parentheses.

method, μ and σ can be obtained from the data series of the normalized peptide percentage and the experimentally determined quantitation ratios of the cICAT-labeled peptide pairs. The cICAT-labeled peptide abundance ratio above which an increase or decrease in abundance should be considered as statistically significant is defined as $-2 \geq z \geq 2$ (*i.e.* 2σ above or below the measured mean ratio). Using these criteria, we determined that the threshold above which a measured cICAT peptide pair abundance ratio reflects a statistically significant increase in abundance should be considered to be >1.645, and the threshold below which a measured cICAT peptide pair abundance ratio reflects a statistically significant decrease in abundance should be considered to be <0.487 for these specific data. Using these criteria 93 proteins were significantly induced, and 37 proteins were significantly repressed in HUVECs responding to 24 h of treatment with sokotrasterol sulfate (Tables I and II, respectively).

To validate this approach, two proteins were chosen, Dysferlin and the transcription factor E2F4, that lie at the threshold of what would be considered significant up-regulation, a 1.75-fold increase (Table I and Fig. 4). Fig. 4*a* illustrates the tandem mass spectra of the observed light and heavy ICAT tryptic peptide $[M + 2H]^{2+}$ isotopomeric ions of Dysferlin. Fig. 4*b* depicts the reconstructed ion chromatograms of the pair of Dysferlin cICAT-labeled peptide molecular ion isotopomers. Similarly Fig. 4*c* shows the tandem mass spectra of the $[M + 2H]^{2+}$ ion of the heavy labeled peptide of E2F4, while the reconstructed ion chromatogram of the cICAT-labeled peptide molecular ions of E2F4 is presented in Fig. 4*d*. We confirmed by immunoblotting that both Dysferlin and E2F4 are up-regulated by sokotrasterol sulfate at 8, 24, and 48 h, and densitometric scanning normalized to a protein that did not change in expression, β-tubulin, demonstrated a similar degree of induction (within the limits of biological and experimental variability) at 24 h as compared with the ratio determined by the extracted ion chromatograms reconstructed from the MS scans (Fig. 5).

To further characterize proteins differentially regulated by sokotrasterol sulfate, proteins were divided according to the

TABLE II
Proteins with decreased expression levels in response to sokotrasterol sulfate

Protein name	Swiss-Prot accession no.	-Fold increase in protein levels[a]
1-Phosphatidylinositol-4,5-bisphosphate phosphodiesterase δ1	P51178	0.42
40 S ribosomal protein S4, Y isoform	P22090	0.17
ADP-sugar pyrophosphatase YSA1H	Q9UKK9	0.31
Amidophosphoribosyltransferase precursor	Q06203	0.41
Branched-chain amino acid aminotransferase, cytosolic	P54687	0.45
CGI-31 protein	Q9Y320	0.35 (2)
Chromatin-specific transcription elongation factor FACT 140-kDa subunit	Q9Y5B9	0.48 (2)
Coronin-like protein p57	P31146	0.22
Cyclin G1	P51959	0.03
CYR61 protein precursor	O00622	0.46
DnaJ homolog subfamily A member 1	P31689	0.28 (2)
Docking protein 1	Q99704	0.39
Dystroglycan precursor	Q14118	0.45
Estrogen sulfotransferase	P49888	0.30
Eukaryotic translation initiation factor 5	P55010	0.04 (2)
Exosome complex exonuclease RRP45	Q06265	0.27
Hypothetical protein FLJ22673	Q9H620	0.43
Hypothetical protein FLJ25701 (similar to RIKEN cDNA 0610011N22)	Q96BQ5	0.44
Hypothetical protein KIAA0564 (fragment)	O60310	0.18
MYB-binding protein 1A	Q9P0V5	0.43
Myc-associated zinc finger protein	P56270	0.45
NDRG1 protein	Q92597	0.39
Nucleoporin-like protein RIP	P52594	0.29
Probable ATP-dependent RNA helicase p47	Q13838	0.36
Proteinase-activated receptor 1 precursor	P25116	0.11
Pumilio 2	Q9HAN2	0.34
Putative polypeptide *N*-acetylgalactosaminyltransferase	Q8NFV9	0.34
Ryanodine receptor 2	Q92736	0.04
SF21 protein	Q8NHE2	0.48 (2)
SMC6 protein	Q96SB8	0.18 (2)
STE20/SPS1-related proline-alanine-rich protein kinase	Q9UEW8	0.45
Structural maintenance of chromosome 1-like 1 protein	Q14683	0.39
Structure-specific recognition protein 1	Q08945	0.32
SWI/SNF chromatin remodeling complex subunit OSA2	Q8NFD5	0.33
Thyroid receptor-interacting protein 6	Q15654	0.43
Tumor necrosis factor receptor superfamily member 1B precursor	P20333	0.05
WAP four-disulfide core domain protein 12 precursor	Q8WWY7	0.10

[a] Number of peptides identified is shown in parentheses.

gene ontology classes of molecular function, cellular compartment, and biological process. Sokotrasterol sulfate-induced proteins in HUVECs are classified in Fig. 6, and down-regulated proteins are classified in Fig. 7. As one would expect in this particular investigation, proteins involved in responding to external stimuli and in cell communication, including cell adhesion molecules, were more likely to be overexpressed than underexpressed in response to sokotrasterol sulfate. Interestingly at least one protein associated with signaling cell death, tumor necrosis factor receptor superfamily member 1B, was down-regulated by sokotrasterol sulfate. The distribution of proteins within cellular compartments was diverse and similar between proteins that were overexpressed and those that were underexpressed except that twice as many membrane proteins were found to be up-regulated, consistent with the gene ontology classification according to biological process. The up-regulated membrane proteins include molecules such as Dysferlin, which to date have not been associated with angiogenesis, as well as other proteins, such as the receptor tyrosine kinase Tie-1 and the α_v integrin subunit, which are both known to be required for vascular development but have not previously been shown to be up-regulated by any steroid molecule (2).

DISCUSSION

Ischemic coronary artery disease is a major cause of morbidity and the leading cause of mortality in the Western world (4). Current therapeutic options for patients with advanced ischemic heart disease include medical therapy or coronary revascularization by percutaneous coronary angioplasty or bypass surgery (4, 18). However, a significant number of these patients are not candidates for standard revascularization procedures or have incomplete revascularization with these procedures. As a result many of these patients have residual

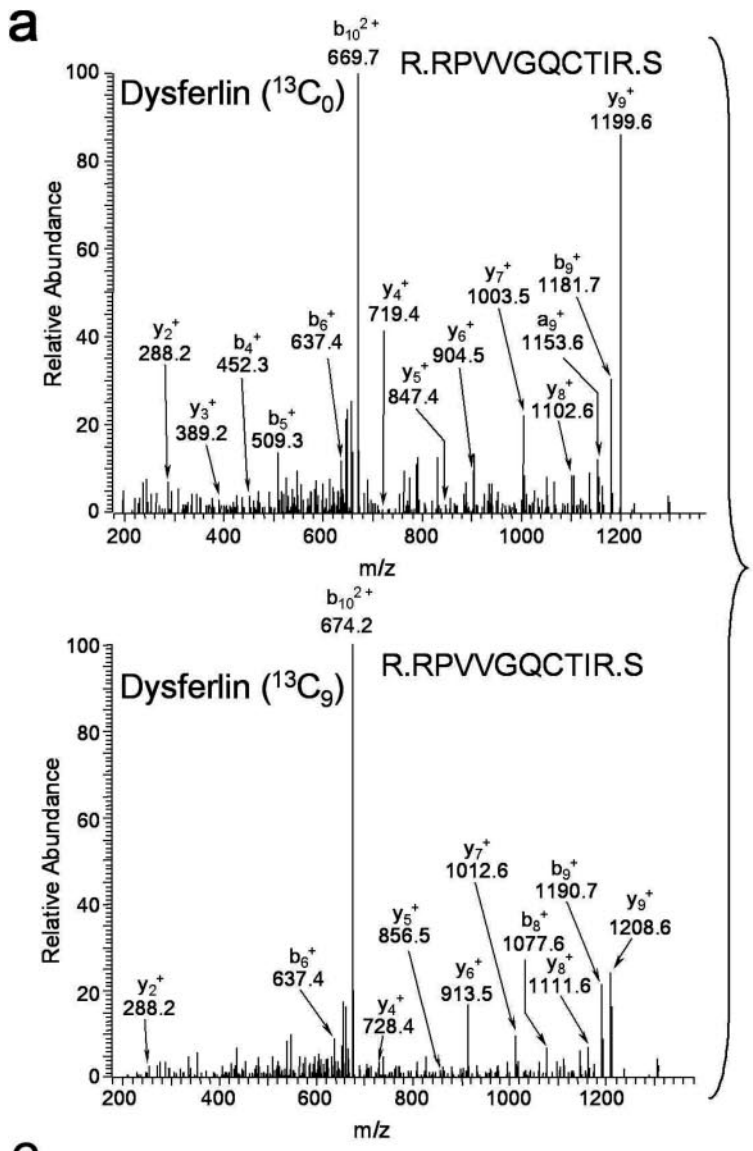

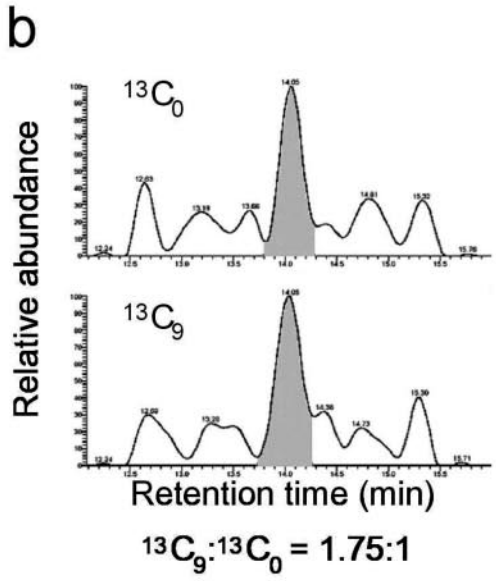

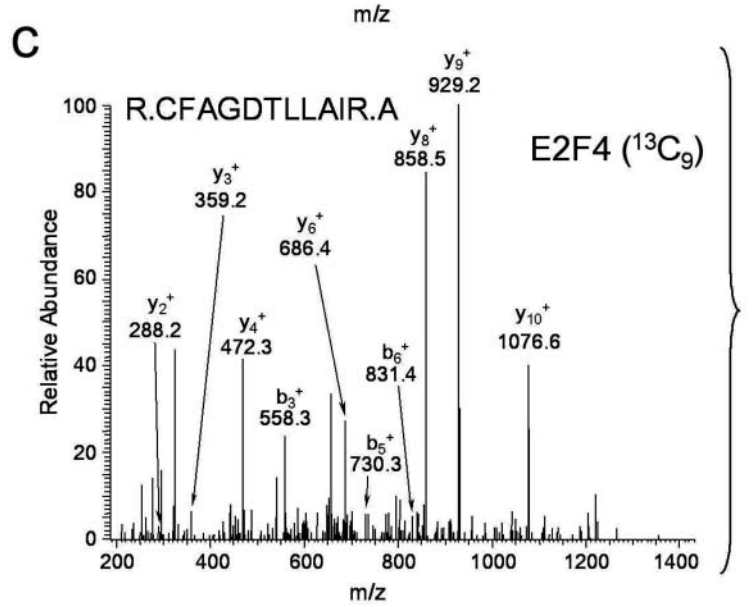

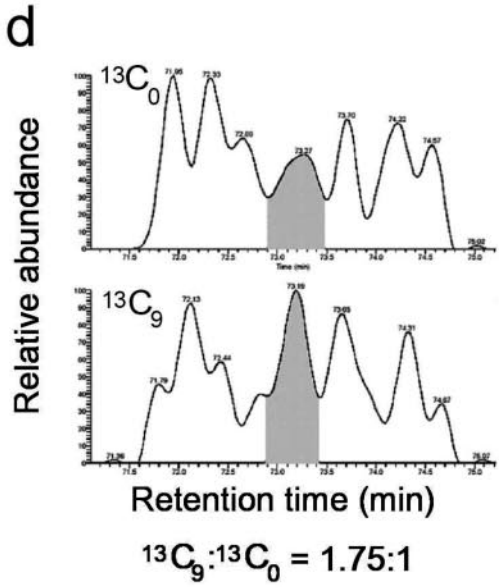

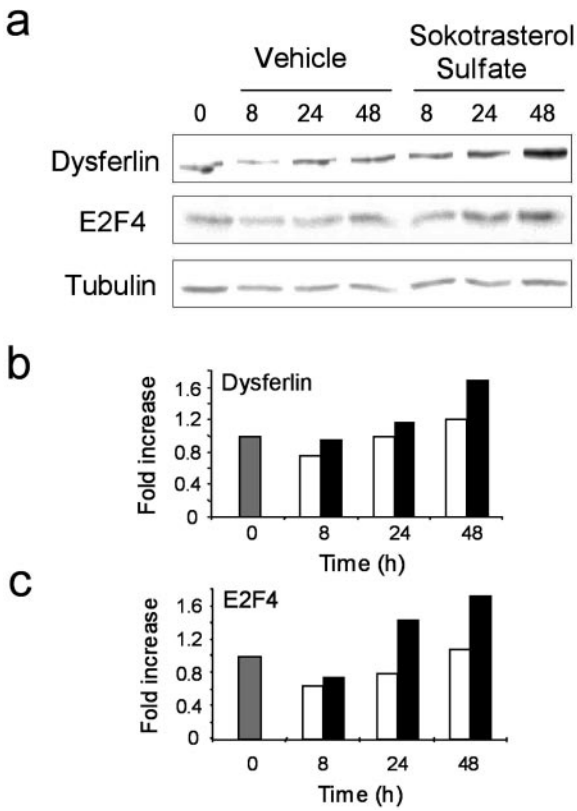

FIG. 5. **Differential expression of representative proteins as determined by immunoblotting.** HUVECs were treated with vehicle or sokotrasterol sulfate (5 μg/ml) for 8, 24, and 48 h as shown. *a*, cell lysates were harvested and subjected to immunoblotting with antibodies directed against Dysferlin, E2F4, or tubulin. Densitometric scans were normalized to tubulin, and the -fold increase in protein expression of Dysferlin (*b*) and E2F4 (*c*), in response to treatment with sokotrasterol sulfate or vehicle, was determined by assigning tubulin-normalized densitometric values in untreated cells (time 0) the arbitrary value of 1.

symptoms of ischemia despite therapy (18). Furthermore the incidence of restenosis or reocclusion in patients who have had invasive revascularization procedures remains distressingly high (18). Hence the ability to promote neovascularization in a non-surgical manner is an important goal (19).

Various steroids have been shown to have either proangiogenic or antiangiogenic activity (14, 20–22). Thus, our discovery of sokotrasterol sulfate as a proangiogenic agent prompted us to elucidate its effects on the expression of proteins potentially involved in angiogenesis. Since the initiating events in angiogenesis are directed at the endothelial cell, we chose to study the effects of sokotrasterol sulfate on differential protein expression in primary endothelial cells.

Consistent with a role in endothelial sprouting and tube formation rather than in proliferation, many of the proteins identified to be up-regulated by sokotrasterol sulfate include molecules associated with cell communication and morphogenesis. For instance CD166/ALCAM, which has not previously been identified in endothelial cells, is reported to be important in directed cell migration, axonal guidance, and branching development (23–25). Our cICAT data showing up-regulation of ALCAM by sokotrasterol sulfate fits well with recent findings demonstrating coordinated events in neuronal and vascular development and shared molecules utilized in the integration of these processes (26, 27). Similarly homeobox proteins are implicated in both vascular and neuronal development (28). In particular the homeoprotein HB9 has been shown to be necessary for axonal pathfinding in a subset of neurons (29). Prior to this study there had been no previous documentation of HB9 being expressed in or involved in endothelial sprouting or angiogenesis. Thus our data showing sokotrasterol sulfate-induced expression of HB9 provides new information to be further investigated in angiogenic experiments.

Interestingly our findings have arisen in a setting where the endothelial cells were cultured in a two-dimensional tissue culture plate, whereas the morphogenic process of vascular sprouting is a three-dimensional process. Up-regulation of the above molecules by differential protein analysis suggests a powerful application for comparative proteomics in modeling *in vivo* events using *in vitro* models. Our data also indicate that some of the findings may be applicable more generally to angiogenesis secondary to other inciting stimuli, while other proteins may be more specific to sokotrasterol sulfate-induced angiogenesis.

The choice of what magnitude of change constitutes a biologically significant increase or decrease in protein expression as measured using ICAT reagents has generally been chosen arbitrarily. Abundance ratios varying from a 1.5- to 2-fold differential increase or decrease have been selected in previous studies to represent a statistically significant change in protein abundance (30, 31). However, such an arbitrary decision may exclude proteins that although not greatly increased in quantity may represent significant changes biologically. On the other hand under certain experimental conditions a 1.5-fold differential expression may not be stringent enough to exclude proteins that do not display a significant change in expression. In this study a statistical method was used to determine the cut-off levels for proteins differentially expressed in response to sokotrasterol sulfate, and we have verified that our cut-off level of ~1.7-fold increase in expression level is reproducible by immu-

FIG. 4. **Differential expression of representative proteins as determined by cICAT analysis.** Shown are representative tandem mass spectra of a peptide derived from control ($^{13}C_0$) and sokotrasterol sulfate-treated ($^{13}C_9$) HUVECs (*a* and *c*). Peptides were identified as RPVVGQCTIR from Dysferlin and CFAGDTLLAIR from the transcription factor E2F4. The cysteinyl residues of these tryptic peptides were covalently modified by the cICAT reagents, allowing for quantitative measurement of the relative abundance of this pair of peptides using XPRESS (*b* and *d*).

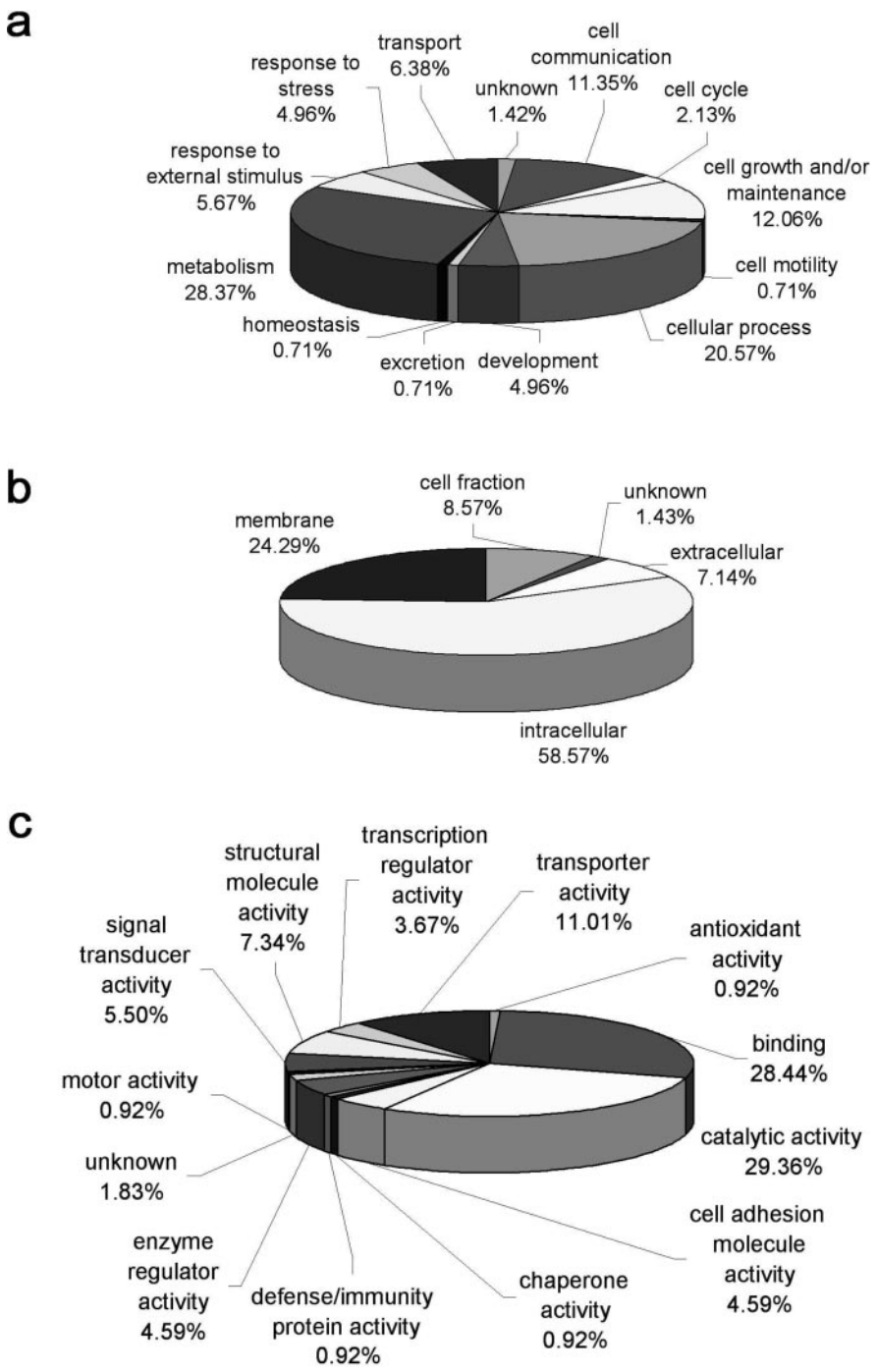

FIG. 6. **Distribution of proteins differentially up-regulated in endothelial cells by sokotrasterol sulfate.** Shown is the classification of proteins according to the gene ontology categories of molecular function (*a*), cellular compartment (*b*), and biological process (*c*).

noblotting. For instance, the up-regulation of E2F4 is consistent with a morphogenic effect of sokotrasterol sulfate. Although transcription factors of the E2F family are known to be necessary for the G_1/S transition during the cell cycle, E2F4 has also been shown to be critical for nerve growth factor-induced differentiation and has been reported to be required for neurite outgrowth independent of cell growth in response to nerve growth factor (32). This finding reveals yet another potential connection between neuronal and vascular development. The second molecule validated, Dysferlin, is expressed on the membrane of skeletal muscle cells and is essential for maintaining the structural stability of the plasma membrane. This protein is mutated in limb-girdle muscular dystrophy and has not previously been shown to be expressed in endothelial cells (33). While the functional relevance of this membrane protein remains to be explored, it is tempting to speculate that Dysferlin may be required to maintain the integrity of the plasma membrane during the migratory phase of angiogenesis where the cell

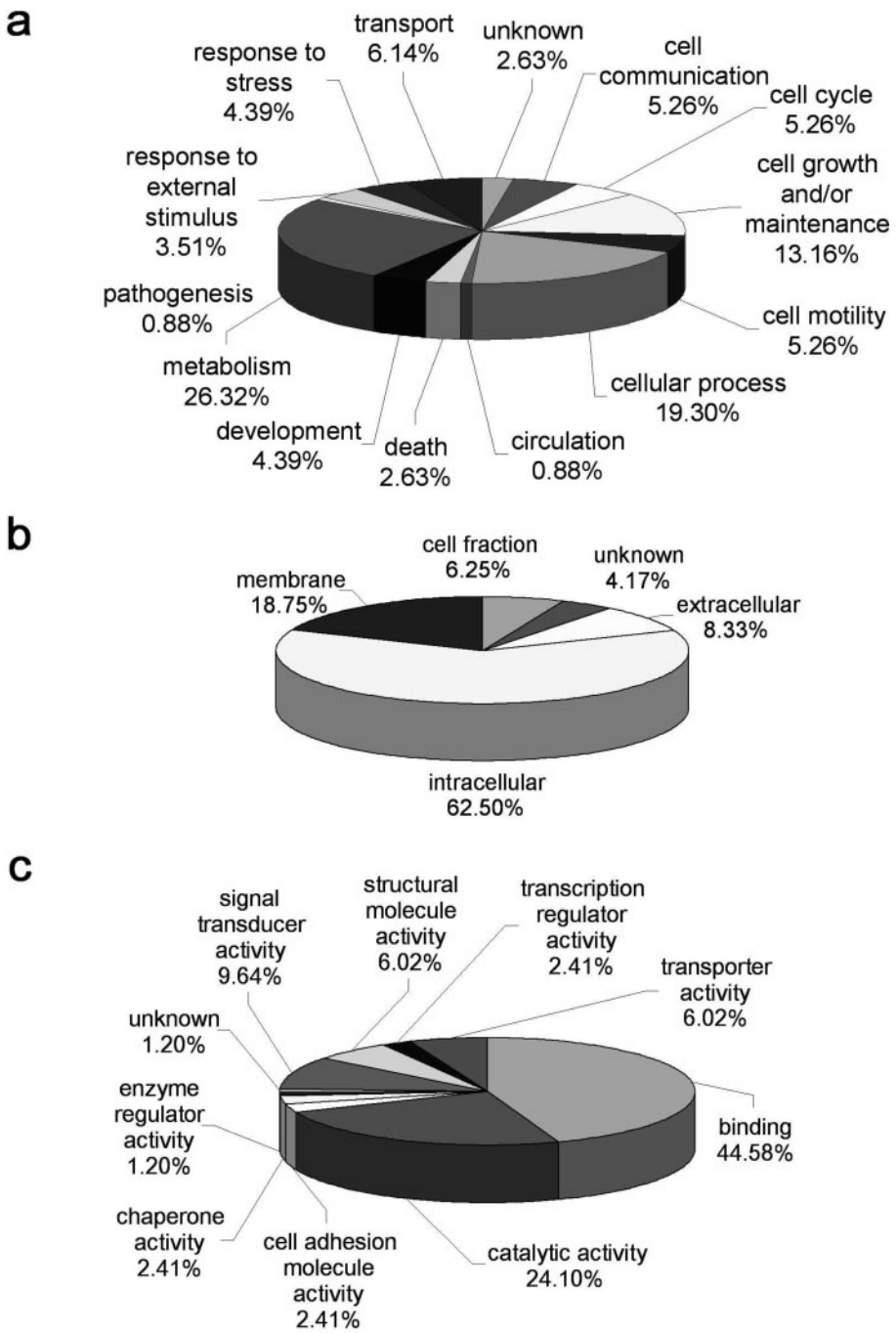

FIG. 7. **Distribution of proteins differentially down-regulated in endothelial cells by sokotrasterol sulfate.** Shown is the classification of proteins according to the gene ontology categories of molecular function (*a*), cellular compartment (*b*), and biological process (*c*).

is actively modulating plasma membrane protein expression and function. Interestingly at least two other proteins that are up-regulated by sokotrasterol sulfate, Tie-1 and α_v integrin, are functionally necessary for angiogenesis (2). Inhibitors against $\alpha_v\beta_3$ integrin are currently undergoing clinical trials as anti-angiogenic therapy in cancer; however, neither $\alpha_v\beta_3$ nor Tie-1 has previously been shown to be up-regulated by any steroid compound (34). These biologically relevant findings would have been missed had a cut-off value of 2-fold increase been chosen. This strategy of determining significantly over- or underexpression thus implicates other proteins at this borderline level that may be potentially important in vascular development.

Very few studies have attempted to undertake global proteomic analysis of endothelial cells (35–38). In addition to differential proteomic analysis that we performed, this is the most extensive global proteomic analysis of primary endothelial cells reported thus far. For instance, in a recent profiling of primary HUVEC cultures using two-dimensional gel electrophoresis, 53 proteins were identified (37). In a more directed approach targeted to identify constituents of

endothelial caveolae and rafts, 25 *bona fide* raft proteins were identified (36). In this study, we identified nine of these 25 raft proteins (36). We also identified multiple other membrane proteins not previously known to be expressed in endothelial cells, such as Dysferlin and ALCAM, thus providing further impetus for the cICAT approach as undertaken in this study.

Finally these findings will be important not only to investigators interested in promoting angiogenesis but also to those involved in inhibiting angiogenesis. Attempts to block angiogenesis to inhibit tumor growth and metastasis have recently proven efficacious in metastatic renal and colon cancer and have provided impetus for a rapid burgeoning of this area of research (39, 40). The identification of molecules that are differentially up-regulated during angiogenesis could provide potential targets toward which antiangiogenic therapeutic agents can be designed.

* This work was supported by grants (to A. K.) from the Heart and Stroke Foundation of British Columbia and the Yukon and the Canadian Institutes of Health Research and in part with federal funds from the NCI, National Institutes of Health, under Contract NO1-CO-12400. The costs of publication of this article were defrayed in part by the payment of page charges. This article must therefore be hereby marked "*advertisement*" in accordance with 18 U.S.C. Section 1734 solely to indicate this fact.

[S] The on-line version of this article (available at http://www.mcponline.org) contains supplemental material.

§ Supported by a personnel award from the Heart and Stroke Foundation of Canada and a scholarship from the Michael Smith Foundation for Health Research. To whom correspondence should be addressed: Dept. of Medical Biophysics, British Columbia Cancer Research Center, Vancouver, British Columbia V5Z 1L3, Canada. Tel.: 604-877-6248; Fax: 604-877-6002; E-mail: akarsan@bccrc.ca.

REFERENCES

1. Carmeliet, P. (2003) Angiogenesis in health and disease. *Nat. Med.* **9,** 653–660
2. Karsan, A., and Harlan, J. M. (1999) in *Hematology: Basic Principles and Practice* (Hoffman, R., Benz, E. J. J., Shattil, S. J., Furie, B., Cohen, H. J., Silberstein, L. E., and McGlave, P., eds) pp. 1770–1782, Churchill Livingstone, New York
3. Folkman, J. (1995) Angiogenesis in cancer, vascular, rheumatoid and other disease. *Nat. Med.* **1,** 27–31
4. Helisch, A., and Ware, J. A. (2000) Therapeutic angiogenesis for ischemic heart disease. *Adv. Exp. Med. Biol.* **476,** 327–350
5. Dor, Y., and Keshet, E. (1997) Ischemia-driven angiogenesis. *Trends Cardiovasc. Med.* **7,** 289–294
6. Ware, J. A., and Simons, M. (1997) Angiogenesis in ischemic heart disease. *Nat. Med.* **3,** 158–164
7. Kutryk, M. J., and Stewart, D. J. (2003) Angiogenesis of the heart. *Microsc. Res. Tech.* **60,** 138–158
8. Celletti, F. L., Waugh, J. M., Amabile, P. G., Brendolan, A., Hilfiker, P. R., and Dake, M. D. (2001) Vascular endothelial growth factor enhances atherosclerotic plaque progression. *Nat. Med.* **7,** 425–429
9. Simons, M., and Ware, J. A. (2003) Therapeutic angiogenesis in cardiovascular disease. *Nat. Rev. Drug Discov.* **2,** 863–871
10. Makarieva, T. N., Shubina, L. K., Kalinovsky, A. I., Stonik, V. A., and Elyakov, G. B. (1983) Steroids in Porifera. II. Steroid derivatives from two sponges of the family Halichondriidae. Sokotrasterol sulfate, a marine steroid with a new pattern of side chain alkylation. *Steroids* **42,** 267–281
11. Cao, Y., O'Reilly, M. S., Marshall, B., Flynn, E., Ji, R. W., and Folkman, J. (1998) Expression of angiostatin cDNA in a murine fibrosarcoma suppresses primary tumor growth and produces long-term dormancy of metastases. *J. Clin. Investig.* **101,** 1055–1063
12. Karsan, A., Yee, E., Kaushansky, K., and Harlan, J. M. (1996) Cloning of a human Bcl-2 homologue: inflammatory cytokines induce human A1 in cultured endothelial cells. *Blood* **87,** 3089–3096
13. Yu, L. R., Conrads, T. P., Uo, T., Issaq, H. J., Morrison, R. S., and Veenstra, T. D. (2004) Evaluation of the acid-cleavable isotope-coded affinity tag reagents: application to camptothecin-treated cortical neurons. *J. Proteome Res.* **3,** 469–477
14. Losordo, D. W., and Isner, J. M. (2001) Estrogen and angiogenesis: a review. *Arterioscler. Thromb. Vasc. Biol.* **21,** 6–12
15. Dabrosin, C., Margetts, P. J., and Gauldie, J. (2003) Estradiol increases extracellular levels of vascular endothelial growth factor in vivo in murine mammary cancer. *Int. J. Cancer* **107,** 535–540
16. Shifren, J. L., Tseng, J. F., Zaloudek, C. J., Ryan, I. P., Meng, Y. G., Ferrara, N., Jaffe, R. B., and Taylor, R. N. (1996) Ovarian steroid regulation of vascular endothelial growth factor in the human endometrium: implications for angiogenesis during the menstrual cycle and in the pathogenesis of endometriosis. *J. Clin. Endocrinol. Metab.* **81,** 3112–3118
17. Washburn, M. P., Wolters, D., and Yates, J. R., III (2001) Large-scale analysis of the yeast proteome by multidimensional protein identification technology. *Nat. Biotechnol.* **19,** 242–247
18. Solomon, A. J., and Gersh, B. J. (1998) Management of chronic stable angina: medical therapy, percutaneous transluminal coronary angioplasty, and coronary artery bypass graft surgery. Lessons from the randomized trials. *Ann. Intern. Med.* **128,** 216–223
19. Sim, E. K., Zhang, L., Shim, W. S., Lim, Y. L., and Ge, R. (2002) Therapeutic angiogenesis for coronary artery disease. *J. Card. Surg.* **17,** 350–354
20. Hasan, Q., Tan, S. T., Xu, B., and Davis, P. F. (2003) Effects of five commonly used glucocorticoids on haemangioma in vitro. *Clin. Exp. Pharmacol. Physiol.* **30,** 140–144
21. Lissbrant, I. F., Lissbrant, E., Persson, A., Damber, J. E., and Bergh, A. (2003) Endothelial cell proliferation in male reproductive organs of adult rat is high and regulated by testicular factors. *Biol. Reprod.* **68,** 1107–1111
22. Mallet, C., Feraud, O., Ouengue-Mbele, G., Gaillard, I., Sappay, N., Vittet, D., and Vilgrain, I. (2003) Differential expression of VEGF receptors in adrenal atrophy induced by dexamethasone: a protective role of ACTH. *Am. J. Physiol.* **284,** E156–E167
23. Ott, H., Diekmann, H., Stuermer, C. A., and Bastmeyer, M. (2001) Function of Neurolin (DM-GRASP/SC-1) in guidance of motor axons during zebrafish development. *Dev. Biol.* **235,** 86–97
24. Fournier-Thibault, C., Pourquie, O., Rouaud, T., and Le Douarin, N. M. (1999) BEN/SC1/DM-GRASP expression during neuromuscular development: a cell adhesion molecule regulated by innervation. *J. Neurosci.* **19,** 1382–1392
25. Swart, G. W. (2002) Activated leukocyte cell adhesion molecule (CD166/ALCAM): developmental and mechanistic aspects of cell clustering and cell migration. *Eur. J. Cell Biol.* **81,** 313–321
26. Park, J. A., Choi, K. S., Kim, S. Y., and Kim, K. W. (2003) Coordinated interaction of the vascular and nervous systems: from molecule- to cell-based approaches. *Biochem. Biophys. Res. Commun.* **311,** 247–253
27. Carmeliet, P., and Storkebaum, E. (2002) Vascular and neuronal effects of VEGF in the nervous system: implications for neurological disorders. *Semin. Cell Dev. Biol.* **13,** 39–53
28. Gorski, D. H., and Walsh, K. (2003) Control of vascular cell differentiation by homeobox transcription factors. *Trends Cardiovasc. Med.* **13,** 213–220
29. Odden, J. P., Holbrook, S., and Doe, C. Q. (2002) Drosophila HB9 is expressed in a subset of motoneurons and interneurons, where it regulates gene expression and axon pathfinding. *J. Neurosci.* **22,** 9143–9149
30. Meehan, K. L., and Sadar, M. D. (2004) Quantitative profiling of LNCaP prostate cancer cells using isotope-coded affinity tags and mass spectrometry. *Proteomics* **4,** 1116–1134
31. Hardwidge, P. R., Rodriguez-Escudero, I., Goode, D., Donohoe, S., Eng, J., Goodlett, D. R., Aebersold, R., and Finlay, B. B. (2004) Proteomic analysis of the intestinal epithelial cell response to enteropathogenic *Escherichia coli*. *J. Biol. Chem.* **279,** 20127–20136
32. Persengiev, S. P., Kondova, I. I, and Kilpatrick, D. L. (1999) E2F4 actively promotes the initiation and maintenance of nerve growth factor-induced cell differentiation. *Mol. Cell. Biol.* **19,** 6048–6056
33. Bansal, D., and Campbell, K. P. (2004) Dysferlin and the plasma membrane repair in muscular dystrophy. *Trends Cell Biol.* **14,** 206–213
34. Folkman, J. (1995) Clinical applications of research on angiogenesis. *N. Engl. J. Med.* **333,** 1757–1763

35. Franzen, B., Duvefelt, K., Jonsson, C., Engelhardt, B., Ottervald, J., Wickman, M., Yang, Y., and Schuppe-Koistinen, I. (2003) Gene and protein expression profiling of human cerebral endothelial cells activated with tumor necrosis factor-α. *Brain. Res. Mol. Brain. Res.* **115,** 130–146
36. Sprenger, R. R., Speijer, D., Back, J. W., De Koster, C. G., Pannekoek, H., and Horrevoets, A. J. (2004) Comparative proteomics of human endothelial cell caveolae and rafts using two-dimensional gel electrophoresis and mass spectrometry. *Electrophoresis* **25,** 156–172
37. Bruneel, A., Labas, V., Mailloux, A., Sharma, S., Vinh, J., Vaubourdolle, M., and Baudin, B. (2003) Proteomic study of human umbilical vein endothelial cells in culture. *Proteomics* **3,** 714–723
38. Kamino, H., Hiratsuka, M., Toda, T., Nishigaki, R., Osaki, M., Ito, H., Inoue, T., and Oshimura, M. (2003) Searching for genes involved in arteriosclerosis: proteomic analysis of cultured human umbilical vein endothelial cells undergoing replicative senescence. *Cell Struct. Funct.* **28,** 495–503
39. McCarthy, M. (2003) Antiangiogenesis drug promising for metastatic colorectal cancer. *Lancet* **361,** 1959
40. Yang, J. C., Haworth, L., Sherry, R. M., Hwu, P., Schwartzentruber, D. J., Topalian, S. L., Steinberg, S. M., Chen, H. X., and Rosenberg, S. A. (2003) A randomized trial of bevacizumab, an anti-vascular endothelial growth factor antibody, for metastatic renal cancer. *N. Engl. J. Med.* **349,** 427–434